Virus Research 339 (2024) 199247

Contents lists available at ScienceDirect

Virus Research

journal homepage: www.elsevier.com/locate/virusres

# Isolation, characterization, and phylogenetic analysis of two new porcine parvovirus 1 isolates from Northern China

Huiwei Deng, Guangyi Cong, Hongfeng Wang, Zedong Hu, Da Shi, Hongyan Shi, Changyou Xia, Fang Fu *, Li Feng *

*State Key Laboratory for Animal Disease Control and Prevention, Harbin Veterinary Research Institute, Chinese Academy of Agricultural Sciences, Harbin 150069, China*

ARTICLE INFO

*Keywords:*
Porcine parvovirus
Complete genome
Phylogeny
Classification

ABSTRACT

Porcine parvovirus (PPV) is a pathogen of infectious reproductive disease, which can cause stillbirth, mummification, embryo death, and infertility (SMEDI) syndrome in pigs. The objective of this study was to gain new insights into the evolution and phylogeny of the PPV1 genome. In this study, we isolated two new PPV1 (HLJ202108-Y and SDLC202109) from northern China and sequenced their whole genomes. The new isolates were found to have three amino acid substitutions (K195R, K562R, and S578P) in nonstructural protein 1. The VP2 amino acid site contained nine nonsynonymous substitutions, including six substitutions of the Kresse strain corresponding to the NADL-2 strain and three substitutions of A414S, S436T, and N555K. Genetic evolution analysis was conducted on 107 reference sequences available in the GenBank database, and 4–5 PPV1 taxa were defined. The new isolates were in the same phylogenetic cluster as strain 27a. The changes in the cluster, specifically marker amino acids, and their potential role in enhancing pathogenicity are discussed in this study. Furthermore, the evolutionary tree map results showed that the strains in China were evolving in two directions: one was becoming increasingly similar to early NADL-2 strains, while the other was evolving toward 27a-like strains. We also compared the proliferation ability of the isolated strains in susceptible cells by analyzing the multistep growth curves. The results showed that the virulence titer of the mutant strain was high. In summary, this study introduced the latest changes in PPV and discussed the virus characteristics that were considered to affect virulence.

## 1. Introduction

Porcine parvovirus (PPV) is an important pathogen that causes reproductive disorders in sows. Clinically, it mainly presents with symptoms of stillbirth, mummification, embryonic death, and infertility, which is called SMEDI syndrome (Cartwright et al., 1969; Dunne et al., 1965; Johnson and Collings, 1969). In recent years, the large-scale infection and rapid prevalence of PPV have led to a significant decline in the reproductive capacity of sows, which has seriously affected the development of the swine industry and resulted in huge economic losses worldwide (Franzo et al., 2023; Parthiban et al., 2022).

The PPV genome, a single-stranded DNA (minus-strand), approximately 4–6 kb in size, is classified in the genus Parvovirus, the subfamily Parvovirinae, and the family Parvoviridae. The genome contains two open reading frames (ORFs). ORF1, located in the left half of the genome, encodes the nonstructural proteins NS1, NS2, and NS3. ORF2, located in the right half of the genome, encodes three capsid proteins, VP1, VP2, and VP3, in which VP3 is the product of VP2 protein hydrolysis (Bergeron et al., 1993; Molitor et al., 1983; Ranz et al., 1989). The two terminal palindrome sequences of the virus form a typical stem ring and hairpin structure with approximately 120 to 200 bases (in a similar "Y" or "T" shape), which is crucial for DNA replication (Astell et al., 1985; Cavalier-Smith, 1974; Cotmore and Tattersall, 1987). However, because of the complexity of the two terminal structures, it is difficult to obtain a complete PPV genome in sequencing work. Non-structural proteins play a role in the cleavage and replication of viral DNA and gene expression regulation (Hanson and Rhode, 1991; Rhode, 1989). In addition, the function of the non-structural proteins involves cytotoxicity, which can induce cell death (Anouja et al., 1997). VP1 and VP2 are the result of alternative splicing of the same gene. The VP2 protein is an important capsid protein of PPV, which is responsible for helping the virus recognize and attach to host cells and establish

* Corresponding authors.
*E-mail addresses:* fangfu@caas.cn (F. Fu), fengli@caas.cn (L. Feng).

https://doi.org/10.1016/j.virusres.2023.199247
Received 14 August 2023; Received in revised form 19 September 2023; Accepted 16 October 2023
Available online 8 November 2023

infection (Bergeron et al., 1996; Simpson et al., 2002). The VP2 region is the main protective antigen, which contains a primary neutralizing epitope and can trigger neutralizing antibodies (De Souza et al., 2019; Kamstrup et al., 1998; Martínez et al., 1992). In addition, an advanced nonstructural protein (SAT) is expressed by the same VP2 mRNA, which activates seven nucleotides downstream of the VP2 start codon (Zádori et al., 2005).

The conservatism of parvovirus may be caused by insufficient PPV monitoring in the 1980s. Field observations until the early 2000s showed that the virus remained stable in terms of immunity (Duffy et al., 2008; López-Bueno et al., 2006; Lukashov and Goudsmit, 2001). However, recent studies have shown that the average substitution rate observed in the PPV genome was close to that of RNA viruses. Parvoviruses have a relatively high evolutionary rate, ranging from $10^{-5}$ to $10^{-4}$ substitution sites$^{-1}$ · year$^{-1}$ (Oh et al., 2017; Ren et al., 2013; Streck et al., 2015; Vereecke et al., 2022). Therefore, it is necessary to further restore and strengthen the pathogen monitoring of PPV to ensure that the developed prevention and control strategies are timely, reasonable, and effective.

In this study, two PPV1 fields strains isolated from northern China (Heilongjiang Province and Shandong Province) were identified and their whole genomes were amplified. The differences in genomic sequence variation sites and amino acid structure were compared and analyzed in detail, revealing their genetic diversity and providing a reference for the study of PPV genetic variation rules and the formulation of effective prevention and control.

## 2. Materials and methods

### 2.1. Cells, viruses, and main reagents

The PPV-BQ strain (GenBank: EU790641.1) was isolated, cultivated, and preserved by the innovation team of pig digestive tract infectious diseases of the Harbin Veterinary Research Institute, Chinese Academy of Agricultural Sciences. The porcine testis cell line (ST) and mouse anti-PPV capsid protein (VP2) monoclonal antibody (1B7 mAb) were prepared and preserved by our laboratory; DMEM with high glucose was purchased from Sigma (China); 0.25 % trypsin-EDTA (1 ×) and RPMI Medium 1640 basic (+ L-Glutamine) were purchased from Gibco; Special fetal bovine serum was purchased from Inner Mongolia Opcel Biotechnology Co., Ltd.; TIANamp Genomic DNA Kit and TIANgel Midi Purification Kit were purchased from Tiangen; DL 2000 DNA Marker, DH5α Competent cell, pMD18-T Vector, and EmeraldAmp PCR Master Mix (2 × Premix) were purchased from TaKaRa (Dalian, China); SafeViewTM FireRed was purchased from ABM; T4 DNA ligase was purchased from NEB (Beijing, China); the 0.22 μm filter was purchased from Merck Chemicals (Shanghai) Co., Ltd.; and AlexaFluor 546 goat anti-mouse IgG antibody (1:200 dilution) was purchased from Thermo Fisher Scientific (China).

### 2.2. Sample collection and processing

Partial samples of the heart, liver, spleen, lung, kidney, and brain tissues of three dead fetal pigs were collected from a pig farm in Heilongjiang Province, China. Another seven dead fetal tissue samples were obtained from a pig farm in Liaocheng City, Shandong Province. After full grinding, an equal proportion of sterilized phosphate-buffered saline (PBS) buffer was added, mixed upside down, and centrifuged at 12,000 rpm for 5 min. The supernatant was used to extract DNA with a DNA virus genome extraction kit.

### 2.3. Virus isolation

PPV-positive supernatant was filtered using a 0.22 μm bacterial filter. When cells were subcultured, the filtrate was added to ST cell culture medium at 1/10 volume and placed in a 37 °C incubator under 5 % $CO_2$. When 90 % of the cells appeared CPE, they were frozen and thawed once. Frozen samples were collected, and the cell suspension was thawed aseptically. It was continued to inoculate new ST cells and was passed 3−4 times until CPE appeared stably. Finally, the harvested cell suspension was detected by PCR to confirm successful separation and stored in the −20 °C refrigerator for standby.

### 2.4. Virus purification and electron microscopic observations

The virus was purified using cesium chloride gradient centrifugation. First, the ST cell culture medium infected by PPV was harvested and centrifuged at 6000 rpm at 4 °C for 30 min to remove impurities. Second, the collected supernatant was centrifuged at 24,000 rpm at 4 °C for 2 h to obtain sediment. The sediment was covered with a sufficient volume of PBS buffer solution and was slowly shaken in the shaker at 4 °C overnight. Third, 2.7 mol/L cesium chloride solution was prepared in an uncapped centrifuge tube. The dissolved suspension was slowly added to the top and ultracentrifuged at 38,000 rpm at 4 °C for 18 h. Finally, the bottom solution was recovered with sufficient PBS buffer and ultracentrifuged at 38,000 rpm at 4 °C for 2 h. The supernatant was discarded, and PBS was added to the bottom part to dissolve the precipitate and obtain purified virus particles. The collected virus particles were sent to the electron microscopy laboratory of Harbin Veterinary Research Institute for electron microscopy observation.

### 2.5. Indirect immunofluorescence assay (IFA)

To determine whether the isolated virus binds the PPV monoclonal antibody, the PPV-infected ST cells were fixed with 4 % paraformaldehyde for 30 min and then permeabilized with 0.2 % Triton X-100 for 20 min. The cells were stained with mouse anti-PPV capsid protein (VP2) monoclonal antibody (1B7 mAb) at 37 °C for 1 h. The bound antibodies were visualized using Alexa Fluor 546 goat anti-mouse IgG antibody (1:200 dilution) (Thermo Fisher Scientific) for 45 min at 37 °C. Cell nuclei were counterstain with DAPI (1 μg/mL) (Sigma-Aldrich, St. Louis, MO, USA). The stained cells were analyzed using an AMG EVOS F1 fluorescence microscope and Leica TCS sp5 confocal microscopy.

### 2.6. Multistep growth curve drawing

The virus solution was inoculated onto ST cells with a cell density of 50 %–60 %, and the ratio of virus solution to medium was 1:7. The old solution was washed-off with RPMI medium 1640 basic 2 h after virus infection. Subsequently, the virus was harvested once every 12 h, and the virus titer ($TCID_{50}$) at each time point was measured for 120 consecutive hours. The multistep growth curve was drawn using GraphPad Prism.

### 2.7. Design and synthesis of whole gene amplification primers

For whole genome amplification, eight pairs of primers (Table 1) were designed for PCR amplification of eight fragments covering the whole genome of the virus. The primer sequences were synthesized at the Harbin Branch of Beijing RuiBiotech. All sequences were performed at least twice to avoid artifacts.

### 2.8. Amplification, cloning, and sequencing of the whole gene

PCR reaction system: EmerldAmp PCR Master Mix (2 × Premium) 25 μL, forward primer (10 μmol/L) 1 μL, reverse primer (10 μmol/L) 1 μL, viral DNA 2 μL, $ddH_2O$ added to 50 μL; PCR reaction conditions: 94 °C for 30 s; 98 °C for 10 s, corresponding annealing temperature for 30 s, 72 °C for 1 min/kb, 30 cycles in total; the final total extension is 10 min.

**Table 1**
List of primer sequences used in this study.

| Fragment | Sequences (5′–3′) | Polarity | Annealing Temperature (°C) | Length of PCR Products |
|---|---|---|---|---|
| P1 | CGC AAT CTT TAA ACT GAC CAA CTG | Sense | 57 | 295 bp |
| | CCA TGC AGT AGC TGA GAG | Antisense | | |
| P2 | CAC TTC GCT CCA GAG ACA C | Sense | 51 | 963 bp |
| | ATC TGT CAT CCA GTC TTC | Antisense | | |
| P3 | CTG AAA CTG TGG AAA CAA CGG | Sense | 53 | 1484 bp |
| | GCT GAG AAG TAG AAG TAT GG | Antisense | | |
| P4 | CGA AGC CTA CGA CAA ATA C | Sense | 54.5 | 1255 bp |
| | TGC TGG TAG TGT TCC TGG GTG | Antisense | | |
| P5 | CTA ACT GAA CCT ACC | Sense | 53 | 923 bp |
| | CAA TGA TAG TAC ATG ATT AAC CAA | Antisense | | |
| P6 | TGG AAC CCT ATT CAA C | Sense | 56 | 425 bp |
| | GTA AAC ACA TGA GAG CTT G | Antisense | | |
| P7 | CAA GCT CTC ATG TGT TTA C | Sense | 55 | 135 bp |
| | AGA GCC GCT TGG TTA GTC G | Antisense | | |
| P8 | TCT GCC GCT TGG TTA GTC GCA CGG | Sense | 55 | 109 bp |
| | GCA ACT AAA CCA ACC ACA CT | Antisense | | |

### 2.9. Phylogenetic analysis

The whole genome sequences of the two isolates were edited and assembled using DNASTAR Lasergene 11 (Madison, Wisconsin, USA). MEGA 11 was used to reconstruct phylogenetic trees using the adjacency method. The phylogenetic tree was calculated using the maximum likelihood method (LG+G + Imodel) with 1000 bootstrap replicates. Information on each reference strain is shown in Table 2.

## 3. Results

### 3.1. Isolation and identification of PPVs

Positive samples containing PPV were inoculated into ST cells, and two strains of the virus were successfully isolated, named HLJ202108-Y and SDLC202109, respectively. Regular icosahedron envelope-free virus particles with a diameter of approximately 20 nm were observed under an electron microscope (Fig. 1). Compared to normal ST cells, infected cells shrunk, were round, and lysed. Further immunological analysis using polyclonal antibodies targeting the PPV1 VP2 protein revealed that the VP2 protein was highly expressed in infected cells (Fig. 2). These results indicated that the new isolates were PPV1.

### 3.2. Comparison of mutant growth curves

As shown in Fig. 3, the growth trend of the isolated strain was relatively fast, reaching a maximum virus titer of $10^{-8.59}$TCID$_{50}$/mL after 72 h of infection. Compared to the PPV-BQ strain, the highest titer difference was nearly 100 times, indicating that the new isolated strain had a higher virus replication level. In addition, Fig. 3(b) indicates that the new isolates had a high hemagglutination titer of 11 units.

### 3.3. Results of whole-genome amplification and sequence analysis

The complete genomes of the isolated strains HLJ202108-Y and SDLC202109 were obtained using a set of primers. The amplification results are shown in Fig. 4. The total length of the two isolates was 4949 nucleotides, and the coding region neither inserted nor deleted. Both isolates contain 127 nucleotide deletions after the VP2 stop codon, as does the virulent strain Kresse. The 5′-UTR hairpin sequence had two base changes, whereas the 3′-UTR hairpin sequence had several base substitutions. The new isolates had three amino acid substitutions (K195R, K562R, and S578P) in non-structural protein 1 using Mega11 for amino acid sequence analysis. Nine nonsynonymous substitutions were identified in the VP2 gene, six of which were consistent with the previously reported Kresse strain (Bergeron et al., 1996), and the other three were A414S, S436T, and N555K.

### 3.4. Genetic analysis and evolutionary results

As shown in Fig. 5, phylogenetic trees were constructed based on the amino acid sequences of the NS1 and VP2 proteins of PPV Based on the phylogenetic relationship of the NS1 amino acid sequence, PPV1 was divided into five groups: A– E. Group A was an early strain represented by the NADL-2 and Kresse strains. Strains with close genetic relationships, such as J-PPV and GD2013, formed the B group, while PPV2010, BQ, and Challenge strains formed the C group. Some strains isolated from the Henan and Nanjing regions of China in the early 21st-century represented the D group. The European and Chinese strains isolated in the past decade were in the E group. The two isolates in this study were classified into the E group, indicating that the NS1 sequence of the new isolate had undergone significant changes compared to the original strain. The evolutionary tree map constructed on the basis of the VP2 amino acid sequence showed that PPV1 was divided into six groups. Early primitive strains, such as NADL-2, were defined as group A. Some strains isolated in the early 21st-century were in group B. The strains represented by Kresse, BQ, and Challenge were classified as group C. Subsequently, some European and Chinese strains in the past decade were finely divided into three groups, D, E, and F, due to their unique residues. The new isolates in this study were in the F group.

## 4. Discussion

Since PPV was first discovered in Europe in the late 1960s, it has contributed to important losses in the swine industry worldwide (Franzo et al., 2023; Gillick, 1977; Johnson, 1973). The first swine parvovirus S-1 strain in China was discovered in 1982, which was followed by the isolation and identification of an increasing number of field strains (Deng et al., 2020; Li et al., 2021). Among them, the PPV-N strain was isolated from the viscera of a stillborn pig in Guangxi, China, in 1989 (Su et al., 2015). The PPV-N strain was also developed as a PPV-attenuated vaccine. A new mutant PPV ne/09 was isolated in 2013, and its 27 nucleotide regions encoding the glycine-rich domain at the n-terminal of VP2 were deleted (Xu et al., 2013). This conservative region is assumed to be the protein hydrolysis cleavage site that produces the smallest capsid protein VP3 (Paradiso, 1984; Rhode, 1985). In addition, the glycine-rich domain is a good selection area for developing molecular probes for the detection and identification of Parvoviridae viruses (Chen et al., 1986; Soares et al., 1999). Phylogenetic analysis showed that the JY strain was the first German-like PPV isolate discovered in China (Hao et al., 2011). More reports indicate that isolated strains, such as PPV2010, J-PPV, and GD2013, have the characteristics of becoming vaccine strains (Cui et al., 2012; Deng et al., 2020; Wang et al., 2014). The BQ strain isolated in 2005 has been developed by our laboratory into an inactivated vaccine that is not yet on the

**Table 2**
Details of the PPV isolates used in this study.

| No. | Isolate | GenBank No. | Collection Date | Country | Dataset |
|---|---|---|---|---|---|
| 1 | NADL-2 | NC_001718 | 1993 | USA | Complete genome |
| 2 | Kresse | U44978 | 1996 | USA | Complete genome |
| 3 | POVCAP | M32787 | 1993 | USA | VP1/2 |
| 4 | POVG | D00623 | 2000 | Spain | NS1 & VP1/2 |
| 5 | 32–96 | AY145472 | 2003 | Brazil | VP2 Partial |
| 6 | 83–95 | AY145473 | 2003 | Brazil | VP2 Partial |
| 7 | 142–95 | AY145474 | 2003 | Brazil | VP2 Partial |
| 8 | 27–00 | AY145477 | 2003 | Brazil | VP2 Partial |
| 9 | 58–00 | AY145478 | 2003 | Brazil | VP2 Partial |
| 10 | 71–00 | AY145479 | 2003 | Brazil | VP2 Partial |
| 11 | 103–95 | AY145480 | 2003 | Brazil | VP2 Partial |
| 12 | 124–95 | AY145481 | 2003 | Brazil | VP2 Partial |
| 13 | 12–97 | AY145482 | 2003 | Brazil | VP2 Partial |
| 14 | 30–95 | AY145483 | 2003 | Brazil | VP2 Partial |
| 15 | 148–95 | AY145484 | 2003 | Brazil | VP2 Partial |
| 16 | 181–95 | AY145485 | 2003 | Brazil | VP2 Partial |
| 17 | 05–95 | AY145488 | 2003 | Brazil | VP2 Partial |
| 18 | 05–96 | AY145489 | 2003 | Brazil | VP2 Partial |
| 19 | 110–95 | AY145490 | 2003 | Brazil | VP2 Partial |
| 20 | 135–95 | AY145491 | 2003 | Brazil | VP2 Partial |
| 21 | 13–97 | AY145492 | 2003 | Brazil | VP2 Partial |
| 22 | 155–95 | AY145493 | 2003 | Brazil | VP2 Partial |
| 23 | 164–95 | AY145494 | 2003 | Brazil | VP2 Partial |
| 24 | 29–97 | AY145496 | 2003 | Brazil | VP2 Partial |
| 25 | 111–00 | AY145499 | 2003 | Brazil | VP2 Partial |
| 26 | 15a | AY684865 | 2006 | Germany | VP1/2 |
| 27 | 21a | AY684868 | 2006 | Germany | VP1/2 |
| 28 | 27a | AY684871 | 2006 | Germany | VP1/2 |
| 29 | 143a | AY684867 | 2006 | Germany | VP1/2 |
| 30 | 106b | AY684870 | 2006 | Germany | VP1/2 |
| 31 | 225b | AY684864 | 2006 | Germany | VP1/2 |
| 32 | IDT | AY684872 | 2006 | Germany | NS1/2/3 & VP1/2 |
| 33 | Tornau | AY684869 | 2006 | Germany | NS1/2/3 & VP1/2 |
| 34 | WB72 | JQ249913 | 2006 | Romania | VP1/2 |
| 35 | WB143 | JQ249914 | 2007 | Romania | VP1/2 |
| 36 | WB533 | JQ249915 | 2010 | Romania | VP1/2 |
| 37 | WB613 | JQ249916 | 2012 | Romania | VP1/2 |
| 38 | WB631 | JQ249917 | 2012 | Romania | VP1/2 |
| 39 | WB639 | JQ249918 | 2012 | Romania | VP1/2 |
| 40 | WB687 | JQ249919 | 2012 | Romania | VP1/2 |
| 41 | WB701 | JQ249920 | 2012 | Romania | VP1/2 |
| 42 | WB716 | JQ249921 | 2012 | Romania | VP1/2 |
| 43 | WB748 | JQ249922 | 2012 | Romania | VP1/2 |
| 44 | WB754 | JQ249923 | 2012 | Romania | VP1/2 |
| 45 | WB773 | JQ249924 | 2012 | Romania | VP1/2 |
| 46 | WB802 | JQ249925 | 2012 | Romania | VP1/2 |
| 47 | WB804 | JQ249926 | 2012 | Romania | VP1/2 |
| 48 | 6R | JQ249927 | 2011 | Romania | VP1/2 |
| 49 | 1h | GQ884035 | 2011 | EU | NS1/2/3 & VP1/2 |
| 50 | 1d | GQ884037 | 2011 | EU | NS1/2/3 & VP1/2 |
| 51 | 3h | GQ884039 | 2011 | EU | NS1/2/3 & VP1/2 |
| 52 | 1f | GQ884040 | 2011 | EU | NS1/2/3 & VP1/2 |
| 53 | 3a | GQ884041 | 2011 | EU | NS1/2/3 & VP1/2 |
| 54 | 2 g | GQ884042 | 2011 | EU | NS1/2/3 & VP1/2 |
| 55 | 6a | GQ884043 | 2011 | EU | NS1/2/3 & VP1/2 |
| 56 | 1g | GQ884044 | 2011 | EU | NS1/2/3 & VP1/2 |
| 57 | 4e | GQ884047 | 2011 | USA | NS1/2/3 & VP1/2 |
| 58 | 7a | JN400516 | 2011 | Germany | NS1/2/3 & VP1/2 |
| 59 | 8a | JN400517 | 2011 | Germany | NS1/2/3 & VP1/2 |
| 60 | 14a | JN400518 | 2011 | Germany | NS1/2/3 & VP1/2 |
| 61 | 693a | JN400519 | 2011 | Australia | NS1/2/3 & VP1/2 |
| 62 | Challenge | AY684866 | 2006 | UK | NS1/2/3 & VP1/2 |
| 63 | 15,425 | JN400520 | 2011 | Switzerland | VP1/2 |
| 64 | VRI-1 | AY390557 | 2003 | South Korea | NS1/2/3 & VP1/2 |
| 65 | T142_Korea | KY994646 | 2017 | South Korea | NS1/2/3 & VP1/2 |
| 66 | HN-Z1 | AY789533 | 2004 | China | NS1 |
| 67 | HN-Z3 | AY789534 | 2004 | China | NS1 |
| 68 | Nanjing-1 | AY739664 | 2004 | China | NS1 |
| 69 | NJ | AY686601 & AY686602 | 2004 | China | NS1 & VP2 |
| 70 | NJ-2 | AY789532 | 2004 | China | NS1 |
| 71 | SD-68 | AY502114 & AY502115 | 2004 | China | NS1 & VP2 |
| 72 | LJL12 | DQ464345 | 2006 | China | VP2 |
| 73 | BQ | EU790641 | 2006 | China | Complete genome |
| 74 | ZJ | EU790642 | 2006 | China | Complete genome |

(*continued on next page*)

**Table 2** (*continued*)

| No. | Isolate | GenBank No. | Collection Date | Country | Dataset |
|---|---|---|---|---|---|
| 75 | China | AY583318 | 2006 | China | NS1 & VP1/2 |
| 76 | SR-1 | DQ675456 | 2006 | China | NS1/2/3 & VP1/2 |
| 77 | HN-2011 | JX992846 | 2008 | China | Complete genome |
| 78 | Nanjing200801 | FJ822038 | 2008 | China | NS1/2/3 & VP1/2 |
| 79 | Nanjing200802 | FJ822039 | 2008 | China | NS1 |
| 80 | S-1 | EU707335 | 2008 | China | NS1 |
| 81 | Tai'an | FJ853420 & FJ853421 | 2009 | China | NS1 & VP2 |
| 82 | PPV2010 | JN872448 | 2010 | China | Complete genome |
| 83 | NE-09 | JQ249926 | 2010 | China | VP2 |
| 84 | JY | HM627652 | 2011 | China | NS1 & VP2 |
| 85 | LZ | HM627653 | 2011 | China | NS1 & VP2 |
| 86 | JT | JN968975 | 2012 | China | NS1 & VP1/2 |
| 87 | GD2013 | KX242359 | 2013 | China | NS1/2/3 & VP1/2 |
| 88 | J-PPV | KF742500.2 | 2013 | China | Complete genome |
| 89 | HNLY201301 | MF447833 | 2013 | China | NS1/2/3 & VP1/2 |
| 90 | HNAY | KJ201927 | 2014 | China | NS1/2/3 & VP1/2 |
| 91 | HNZK-1 | KJ201928 | 2014 | China | NS1/2/3 & VP1/2 |
| 92 | HuN1 | MH183298 | 2015 | China | NS1 & VP1/2 |
| 93 | PPV1-DJH11 | MK092380 | 2015 | China | NS1 & VP1/2 |
| 94 | PPV1-DJH22 | MK092382 | 2015 | China | NS1 & VP1/2 |
| 95 | PPV1-DJH23 | MK092383 | 2015 | China | NS1 & VP1/2 |
| 96 | PPV1-DJH24 | MK092384 | 2015 | China | NS1 & VP1/2 |
| 97 | N | HM989009 | 2015 | China | NS1/2/3 & VP1/2 |
| 98 | TJ | KX233726 | 2016 | China | Complete genome |
| 99 | China-XY | MK993540 | 2017 | China | Complete genome |
| 100 | JSYZ20170418–30 | MZ577026 | 2017 | China | NS1/2/3 & VP1/2 |
| 101 | SDQD20200424–830 | MZ577027 | 2020 | China | NS1/2/3 & VP1/2 |
| 102 | CH/HN-3/2021 | MZ677266 | 2021 | China | NS1/2/3 & VP1/2 |
| 103 | CH/HN—H/2021 | MZ706996 | 2021 | China | NS1/2/3 & VP1/2 |
| 104 | BJ2 | OP235938 | 2022 | China | NS1/2/3 & VP1/2 |
| 105 | SDPV1 | ON924737 | 2022 | China | Complete genome |
| 106 | SDPV2 | ON924738 | 2022 | China | Complete genome |
| 107 | SDPV3 | ON924739 | 2022 | China | Complete genome |

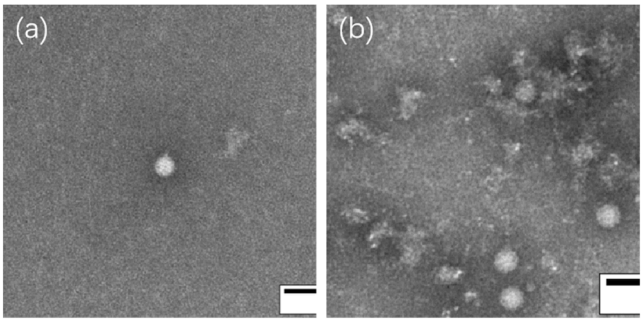


**Fig. 1.** PPV-1 infection in ST cells. (a) Negative staining electron micrograph of PPV1-HLJ202108-Y virus cultured in ST cells. (b) Negative staining electron micrograph of PPV1-SDLC202109 virus cultured in ST cells.

market (Shangjin et al., 2009).

In this study, two PPV1 strains were isolated from northern China and their genomes were amplified. The HLJ202108-Y strain was isolated from the brain tissue of aborted fetuses in a commercial pig farm in Heilongjiang Province, China. The SDLC202109 strain was detected in the liver tissues of stillborn fetuses on a pig farm in Liaocheng City, Shandong Province. Both of them contain 4949 nucleotides, with a G + C content of 38.31 %, The homology of the HLJ202108-Y strain with the NADL-2 strain and Kresse strain was 99.3 %, while that of the SDLC202109 strain with two classical strains was 99.2 %. Sequence alignment revealed no insertion or deletion in the coding region of the two new isolates. Consistent with the virulent strain Kresse, there was no 127-nucleotide repeat in the right-hand ORF. On the evolutionary tree map constructed with the VP2 gene, two viruses formed a small branch in Group F.

The hairpin structure of parvovirus plays a central role in its DNA replication process, and the size of the hairpin, changes in nucleotides, and prediction structure may change the stability of the structure, thus affecting the replication of viral DNA and possibly affecting the biological characteristics of the virus (Hanson and Rhode, 1991). However, a recent study on the protein secondary structure of Canine parvovirus shows that the spontaneous generation right hairpin mutation of three Canine Parvovirus genotypes has no significant effect on their growth characteristics (Yu et al., 2019). Due to the complexity of the hairpin structure, it is difficult to obtain palindrome terminal sequences through ordinary PCR technology, and there are few complete PPV1 genome full-length hairpin sequences in the GenBank database; therefore, few studies have been conducted on the hairpin structure. Although the 5′-terminal hairpin sequences obtained from the existing sequence have a high degree of conservation, ours had two base changes (A142G, G264A). Meanwhile, we found nine base differences and one base insertion in the 3′ end hairpin sequence. The impact of changes in the hairpin structure of isolates on the replication of viral DNA and their role remains to be established.

The main nonstructural proteins NS1 and NS2 of PPV are related to the early and late transcription of the virus. Although they do not directly participate in the assembly of viral particles, they play an important regulatory role in virus replication (Fernandes et al., 2014). The phylogenetic analysis of the NS1 protein sequence showed no significant difference in the amino acid composition of the NS1 protein between the NADL-2 and Kresse strains, although this has received less attention in this field in the past. Vasudevacharya et al. (Vasudevacharya and Compans, 1992) used the PPV mutant P2 to demonstrate that a mutation in the NS gene was sufficient to alter the important biological characteristics of the virus, i.e., its host range.

Table 3. Grouping and polymorphic sites along 63 complete PPV NS1 amino acid sequences compared to the NADL-2 strain. The dots indicate amino acid identity (Table 3 is given in the appendix).

The result of comparing the 63 NS1 protein sequences collected in this study revealed 77 polymorphic sites out of 662 amino acid sites (Table 3). When comparing the new isolates in this study with the NADL-

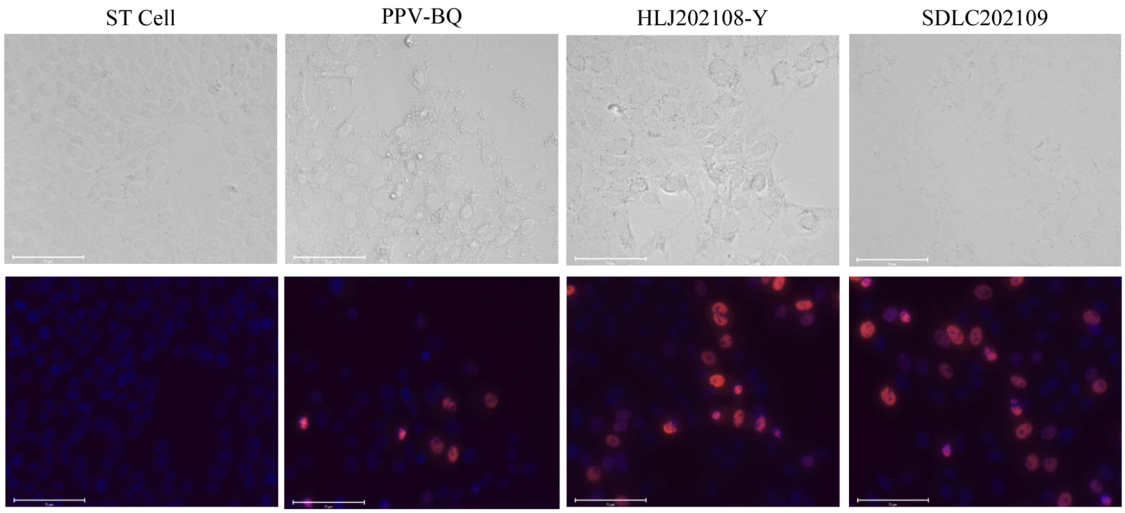


**Fig. 2.** PPV strains HLJ202108-Y and SDLC202109 with control (virus and cell) replicated in ST cells. The upper and lower panels show light and the corresponding immunofluorescent microscope images, respectively, of ST cells infected with the PPV strains. PPV-infected ST cells were fixed at 1 PID. PPV and nuclei were detected with mouse anti-PPV VP2 protein monoclonal antibody 1B7 and 4′,6-diamidino-2-phenylindole (DAPI), respectively (red for PPV antigens, and blue for nuclei).

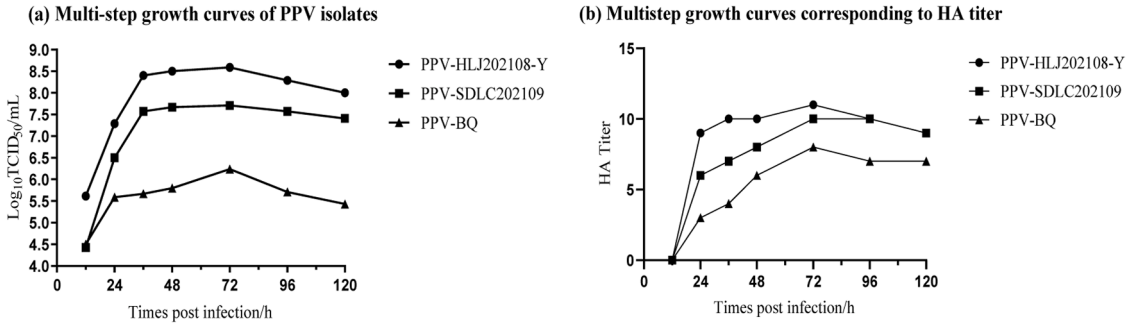


**Fig. 3.** (a) Multistep growth curves of PPV isolates; (b) multistep growth curves corresponding to the HA titer.

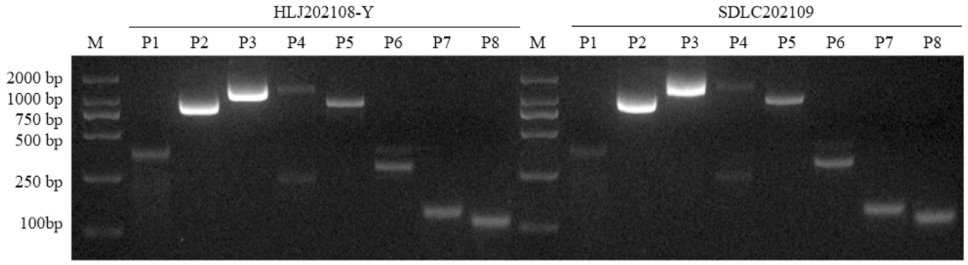


**Fig. 4.** Whole genome amplification of PPV isolates.

2 strain, three amino acid substitutions (K195R, K562R, and S578P) were found in the newly isolated strains. Amino acid 562 and 578 are also located in the NS2 protein, while S578 is a new discovery. The previous change in residue 578 only occurred in the S-1 strain (S578A). Residues 195 and 562 are important sites in the NS1 gene. K195R distinguishes PPV1 from the AB group and other groups, whereas K562R mainly exists in strains in group E. It remains unclear whether the substiution of three amino acids in our strains has an impact on virus replication.

Additionally, on the NS1 evolutionary tree map (Fig. 5a), we found the following residue sites, which distinguished the groups of the virus strains: G242S was widely present in the NS1-D and VP2-B groups; S358G mainly appeared in some strains of the NS1 E group and VP2 E and F groups; N513H was mainly characterized by most strains in the NS1-B group; and A544S and M568I were commonly found in strains isolated from the Henan and Nanjing regions of China in the early 21st century, located in the NS1-A and VP2-B groups. Mutations in K562R, D590N, and I633V mostly occur in the NS1-E and VP2-F groups, and the isolation time of the virus strains in these two groups is the closest to that currently. Some of these are also described in the classification of four groups by Hao et al. (Hao et al., 2011). Additionally, when analyzing a hypothetical non-structural protein NS3, 10 polymorphic sites were found among 107 amino acids, with Val55 showing the greatest difference. The roles of these sites in pathogenicity are not yet clear.

VP1 and VP2 are important capsid proteins of PPV, which are translated from a nested variant of the VP1 protein, albeit with different amino-terminals (Bergeron et al., 1996). The analysis of 150 unique amino acids in VP1 showed that the fragment of all reference strains was generally conserved, with only the POVG strain showing significant differences, with 21 more amino acids at the N-terminus compared to

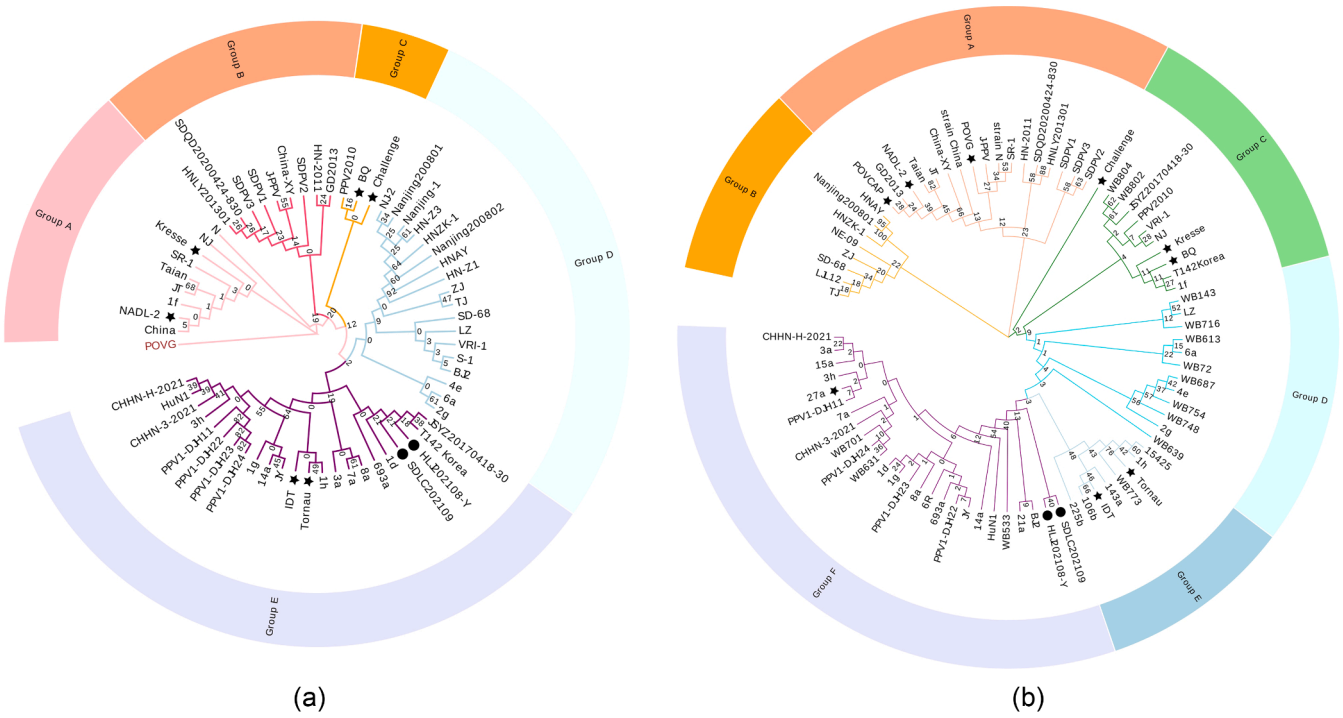


**Fig. 5.** A phylogenetic tree constucted on the basis of two datasets. (a) PPV1 was divided into five groups based on the NS1 protein sequence. (b) PPV1 was divided into six groups based on the VP2 protein sequence.

other strains. The experimental results of Kamstrup et al. revealed that the peptide from the VP1-unique region, composed of 150 amino acids, cannot induce PPV to produce neutralizing antibodies (Kamstrup et al., 1998). The VP2 protein contains virulence-determining factors that can help the virus recognize and bind to the host cell nucleus and establish infection (Bergeron et al., 1993). Previous studies have found six differences in the 579 amino acids of the VP2 protein between NADL-2 and Kresse strains (T45S, I-2153T, D-378 G, H-383Q, S-436P, and R-565 K), which may explain the differences in PPV tropism, host range, and coagulation characteristics (Bergeron et al., 1996).

Table 4. Grouping and polymorphic sites along 82 complete PPV VP2 amino acid sequences compared to the NADL-2 strain. Dots indicate amino acid identity. The deletion of the NE-09 strain at loci 27–35 and the addition of a threonine between sites 365 and 366 in strain TJ are not shown in the table. gray-marked residues correspond to the positions responsible for differences between the NADL-2 and Kresse strains of PPV (45, 215, 378, 383, 565) (Table 4 is given in the appendix).

To further investigate the relationship between VP2 amino acid diversity and phylogenetic development, we analyzed 82 VP2 protein sequences, including two newly isolated strains, and detected 85 polymorphic loci (Table 4). In this study, these two new isolates not only contained amino acid substitutions consistent with the Kresse strain, but also three non-synonymous mutations, namely A414S, S436T, and N555K. These three sites may be related to the virulence and hemagglutination characteristics of the virus. Because differences were found in the TCID50 values and hemagglutination titer between the BQ strain and the new isolates (Fig. 3), only these three differences were found on VP2 between strain BQ and the new strains (proline at position 436 of BQ replaced serine). We also observed similar changes in amino acid residues at sites 414 and 436 of strains 27a and 143a, which may indicate that the newly isolated strains have biological characteristics similar to those of the 27a strain and are also 27a-like strains. Zeeuw et al. (Zeeuw et al., 2007) observed virus titers of $10^{5.1}$, $10^{4.9}$, $10^{6.9}$, and $10^{6.5}$ TCID50/ml for 27a, NADL-2,143a, and IDT, respectively. In the pathogenicity test conducted by Mengeling et al. (Mengeling, 1979), the $TCID_{50}$ of NADL-8 was $10^{6.7}$ $TCID_{50}$/mL. Animal experiments conducted by Molitor et al. (Molitor et al., 1983) showed that the $TCID_{50}$ of the NADL-8 virulent strain was $10^7$ $TCID_{50}$/mL. The highest $TCID_{50}$ titer of the two new isolates in this study reached $10^{8.59}$, which may indicate that these two new isolates have higher replication ability on cells. Changes containing 555 amino acid residues occurred in POVG, IDT, 106b, SR-1, PPV2010, J-PPV, and PPV-N strains, which had been identified as attenuated strains. However, their amino acids at positions 414 and 436 were still different from those of the new isolates, which may indicate that the changes at the 555 loci do not have a greater impact on virulence expression than the first two.

A recent study suggested that the Thr45 site may be related to certain characteristics of low-virulence PPV strains and can be used to identify low-virulence strains as candidate vaccines (Deng et al., 2020). On the evolutionary tree map of VP2 (Fig. 5b), we can see that Thr45 distinguished low virulence strains such as POVCAP, GD2013, NADL-2, Taian, JT, China-XY, China, and J-PPV within Group A. As a small branch in Group F, the new isolates may not be low virulence strains because they possessed the Thr45 characteristic.

The amino acid at position 215 was located at the base of the capsid subunit, and the isoleucine and threonine at position 215 distinguished the strains of Group AB from those of other groups. This position at the triple spike is considered an important antigen surface region of various parvoviruses (Chapman and Rossmann, 1993). The characteristics of two new strains Thr215 may have altered the adaptability of the strain compared to the NADL-2 strain, which is the same change as that observed in the Kresse and 27a strains.

Amino acids 378, 383, and 565 are in the double depression of the capsid subunit, which is sufficient to alter the phenotype of parvovirus (Bergeron et al., 1996). The amino acids 378, 383, and 565 were all in a positive selection state which were shown in previous studies to suggest that amino acid changes at these sites may be beneficial for the survival of PPV (Cadar et al., 2012; Ren et al., 2013; Streck et al., 2015, 2011). The amino acids around position 378 were found to be neutralizing epitopes similar to the strain 27a by Streck et al. (Streck et al., 2022). These three residues are believed to be involved in the immune response, and research results on PPV-27a, PPV-143a, PPV-Challenge,

and PPV-IDT suggest that these three sites are unlikely to determine pathogenicity (Zeeuw et al., 2007). Subsequent *in vitro* experiments reported that S436P was not involved in tissue tropism (Fernandes et al., 2011). Asp378, His383, and Arg565 are widely present in group A and B strains, similar to Thr45, and that these strains were mostly present around the year 2010.

As the position with the greatest mutation pressure, amino acid 436, located at the center of the three-fold peak of the capsid subunit, is the most accessible capsid structure, which is related to cell tropism (Bergeron et al., 1996; Simpson et al., 2002). This region corresponds to the epitope B of feline parvovirus (Strassheim et al., 1994) and plays a role in reducing the affinity of PPV neutralizing antibody (Zeeuw et al., 2007). The high mutation rate of amino acids at this position provides some adaptive advantages for the virus. The amino acid at position 436 has mutated from the beginning of serine to alanine, proline, threonine, and aspartic acid. The VP2 evolutionary tree graph (Fig. 5b) demonstrates that the Ala436 strains have widespread characteristics of group B strains (except for NE/09), while some strains of group D (WB143, LZ, WB613, 6a, WB72, WB639) have also been found. Ser436 is a characteristic of these early PPV strains in group A. Pro436 is a characteristic of the C group and some E group strains. Thr436 is a common characteristic of F group strains represented by 27a-like strains. Asp436 is only found in strains IDT, 106b, and the recently emerged strain BJ2.

The substitution of other residues on VP2 cannot be ignored. The residues 226, 228, 320, 419, and 423 are located near the triple shoulder of the capsid subunit (Simpson et al., 2002). Q228E is a characteristic of strains WB639, WB773, and group F (excluding strains HLJ-Y202108 and SDLC202109), and this position has been identified as part of one of the nine known linear epitopes on VP2 (Kamstrup et al., 1998; Simpson et al., 2002). I320T is widely present in the strains of groups A and B, most Brazilian isolates studied by Martins Soares et al. in 2003, and all strains of group E. In addition, I320S/M showed specificity in the strains China-XY and VRI-1, respectively. E419Q is a characteristic of SDPV1–3, 1 h, 225b, and F group strains (excluding strains HLJ-Y202108 and SDLC202109). N423K/T only appeared in Brazilian isolates and TJ strains. Thr233 and Thr304 are located at the triple-pointed protrusion center of the capsid subunit, and this mutation occurs almost exclusively in the E-group strain, which may provide some adaptive advantages for members of the group. In addition, some subbranches of groups B and D contain Thr233. R82K has also been observed in CPV and is a characteristic of SDPV2, SDPV3, and all E-group strains. This site may be related to cell specificity and hemagglutination activity (Chapman and Rossmann, 1993).

Moreover, by analyzing amino acid polymorphism sites and VP2 evolutionary tree maps, we observed many phenomena, including the fact that E144A mainly occurred in strains of group A, L391V was found only in group B strains, and all group E strains contained mutations in T20A and K407N. Group F strains were widely mutated from alanine to serine at position 413, whereas strain BJ2 was threonine. Mutations in Q302L, A372T, N397T, N423T, H439N, M441T, E551D, I54M, and N555R/H mainly occurred in early Brazilian isolates (Soares et al., 2003). These results are consistent with those of Hao et al., 2011).

Although we have observed these mutations, their biological consequences are not entirely clear. The latest research results reveal that when a single T45S or E419Q mutation occurs, the virus strain cannot produce sufficient viral titers after transfection. With the exception of the independent R565K mutation, the remaining individual residue mutations of I215, Q228E, D378G, H383Q, A414S, and S436T resulted in the mutant exhibiting higher adaptability to cells than the non-mutant. The monoclonal antibody Mab-9A5 can neutralize mutants containing D378G, H383Q, A414S, S436T, and R565K substitutions but cannot neutralize viruses containing I215T, Q228E, I215T+Q228E, and A414S+E419Q+S436T substitutions, suggesting that there may be some synergistic effects between various loci (Streck et al., 2022). Further research is needed on the impact of more residues on the capsid structure and pathogenicity, and whether they are involved in immune escape.

In the past, some scholars have proposed rich insights into classification and evolution in the phylogenetic analysis of PPV.

Zimmermann et al. (Zimmermann et al., 2006) defined two genetic lineages of PPV strains based on their analysis of the VP1 sequences of eight strains from Germany in 2006. The three strains 15a, 27a, and 21a form a cluster, whereas strains 143a, 225b, Tornau, IDT, and 106b form another cluster. We can see consistent results on the VP2 evolutionary tree map of this study, with strains 15a, 27a, and 21a located in the classified Group F, and several other German strains all located in group E.

The research results of Shangjin et al.(Shangjin et al., 2009) showed that regardless of whether NS1 or VP2 genes were used as the basis for analysis, PPV1s could be divided into two major groups, each with two branches. These classifications and branches were highly consistent with our antigen spectrum. For the “highly, medium, and attenuated” strains of PPV described by Shangjin, we found limited correlation in their scattered branches of the evolutionary tree, as each type of strain was dispersed across various groups.

Hao et al. (Hao et al., 2011) divided PPV strains into four groups in 2011. The early Chinese PPV strains were group I viruses, whereas almost all subsequent Chinese PPV strains were group II viruses. On the evolutionary tree map of this study, PPV I was mainly located in groups A, B, and C, classified by NS1, and in groups A and C, classified by VP2, representing some early PPV isolates. Class II PPVs are in the NS1-D and VP2-B groups, respectively, representing some viruses with more mutations in the decade at the beginning of the 21st-century. Class III and IV PPV mainly appear in groups D, E, and F. Some 27a-like viruses and new isolates developed recently belong to these two groups.

This phylogenetic study has led to the identification of new information. The graph in Fig. 5 showed that the isolates in China have been developing in two directions in the past 5 years. One was represented by the BJ2 strain, PPV1-DJH series, and CHHN series, which were evolving in the 27a-like direction, while the SDQD2020 and SDPV series strains were increasingly similar to the early strains and were recovering from the original strains isolated more than 30 years ago. This viewpoint is consistent with the research of Woo-Taek Oh et al. (Oh et al., 2017). Additionally, Woo-Taek Oh et al. mentioned the Asian lineage of PPV was completely different from its European lineage, forming its own evolutionary branch. Indeed, this was confirmed on the VP2 evolutionary tree map (Fig. 5b), where the strains of A to C groups are mainly from North America and China, while the strains of D to F groups are mainly from Europe. Similar findings were found in the latest study by Vereecke et al. (Vereecke et al., 2022). In terms of time, the A-C group strain was isolated earlier, whereas the European strain was isolated relatively late, which may indicate that global PPV1 is generally evolving toward 27a-like.

The repeat sequence of the ORF2 coding structural proteins VP1 and VP2 127b downstream, of PPV may have some connection with the virulence of PPV. The tandem repeat sequence may be important for the replication of the virus genome, and this region may interact with the inner surface of the capsid, thus affecting DNA encapsidation (Fernandes et al., 2011; Zeeuw et al., 2007). The replication level of MVMp lacking a duplicate sequence copy in A9 cells is approximately 10% of that of wild-type viruses. Furthermore, the number of repetitions can affect the stability of the transcript (Sachs, 1993). We observed that most PPV strains only had two situations, either containing 127 base repeats, as in the NADL-2 strain, or missing such repeats like the Kresse strain. However, as shown in Fig. 6, we found several “unique” sequences, among which, strain Nanjing200801 showed the longest sequence, adding nine bases at the end of the 127 repeat sequences, as well as containing 58 repeat sequences in front of the repeat, with a difference starting from the 41st base. HNZK-1 also contained these 58 base repeat sequences, but 45 bases are missing in the subsequent 127 repeat sequences, similar to that in the HNAY strain, which is different from the previously discovered deletions in BQ and ZJ strains. Similarly, MVMi (a

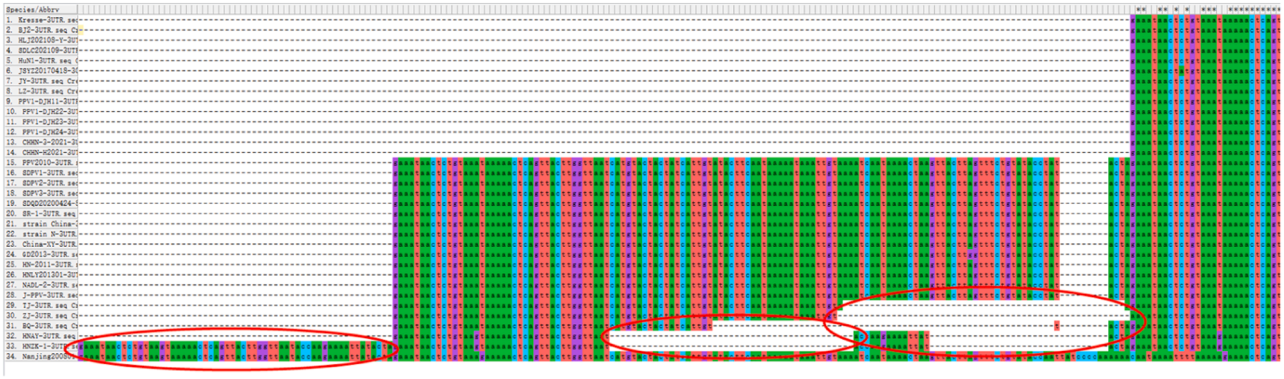

**Fig. 6.** Alignment analysis of the terminal sequences of PPV strains.

lymphatic variant of MVM) also lacks a 65 bp repeat sequence (Astell and Chow, n.d.). We are not yet clear about the performance of these differences in the virus as it is difficult to determine the virulence of the strains solely on the basis of the length of repeat sequences. Although IDT and 143a lacked the repeatability of 127 nt, they seemed to have no pathogenicity. The latest research by Streck et al. (Streck et al., 2022) shows that when using strain Kresse with only a 127 nucleotide repeat as the parent strain to construct mutants, these mutants cannot recover from infectious viruses after transfection or replicate at an efficiency that allows for further analysis.

Another interesting point is that the strains with 127-nt repeats were mostly located in groups D, E, and F. The strains with unique replicates were mainly located in group B (excluding BQ and IDT). When conducting amino acid analysis on VP2, we found that the group B strains had the most amino acid mutations, which is why they were classified into a large group. They not only exhibited unique mutations on VP2 (including 36 strains of group A among the 85 amino acid polymorphism sites in VP2) but also exhibited diversity in the 127 nt repeat region. Therefore, we speculated whether there was a correlation between mutations in the VP2 region and duplication of 127 nt. A 2011 study by Fernandes et al. (Fernandes et al., 2011) showed that the interaction between the NS1 protein and the VP gene involved interactions with non-coding repetitive sequences. The latest discovery by Streck et al. (Streck et al., 2022) indicates that most amino acid substitutions alter the replication efficiency of the strain. However, this is not the case when multiple mutations are inserted into the virus. This may suggest that when we study the virulence difference of PPV, we should not only look at the change of a certain site in the VP2 region but also look at the NS gene, VP gene, and noncoding repetitive sequence together.

The genetic diversity of PPV is more extensive than before. The new isolates have similar but incomplete amino acid substitutions at the VP2 site as the 27a strain, which may indicate certain changes in the immune level of the new isolate. However, further testing is required for specific validation, which poses a challenge to the effectiveness of current vaccines. Although inactivated and attenuated vaccines are widely used in pigs, PPV infection remains a serious infectious disease. Learning from the research on the PPV vaccine market in Heilongjiang Province of China, two inactivated vaccines, the S-1 and WH-1 strains, are mainly sold in the market. These two vaccines have been in use for nearly 20 years. Although some pig farms have been vaccinated with PPV vaccines, but the clinical symptoms of abortion and stillbirth still occur, which poses a challenge to the effectiveness of the vaccine. It is necessary to design a new vaccine to prevent a new PPV epidemic. Therefore, it is essential to conduct PPV surveillance and strengthen research on the genome evolution of PPV1 epidemic strains.

In summary, we isolated two virulent strains of PPV type 1, obtained their complete sequences, and described their genomic characteristics. The amino acid polymorphism sites of PPV have evolved from a few in the early years to nearly 100 now. This article states that some new frequently replaced loci are gradually coming into the public's view. The purpose of this study was to expand the phylogenetic insights of PPV and provide further data for the evolution of the virus, as well as references for the classification of type 1 subgroups. Although PPV still causes reproductive disorders in sows at the macro level, changes in amino acid sites may lead to microscopic differences at the molecular level.

## Declaration of generative AI in scientific writing

The authors declare that no artificial intelligence and artificial intelligence-assisted technologies were used during the writing process.

## CRediT authorship contribution statement

**Huiwei Deng:** Conceptualization, Methodology, Software, Investigation, Formal analysis, Data curation, Validation, Visualization, Writing – original draft. **Guangyi Cong:** Methodology, Writing – review & editing. **Hongfeng Wang:** Resources, Supervision. **Zedong Hu:** Methodology, Writing – review & editing. **Da Shi:** Software, Resources. **Hongyan Shi:** Resources. **Changyou Xia:** Funding acquisition, Resources. **Fang Fu:** Project administration, Conceptualization, Methodology, Formal analysis, Funding acquisition, Resources, Supervision, Validation, Writing – review & editing. **Li Feng:** Project administration, Resources, Supervision, Funding acquisition.

## Declaration of Competing Interest

We declare that we have no financial and personal relationships with other people or organizations that can inappropriately influence our work, and there is no professional or other personal interest of any nature or kind in any product, service, and/or company that could be construed as influencing the position presented in, or the review of, the manuscript entitled.

## Data availability

The complete genome sequence of the PPV isolate HLJ202108-Y has been deposited in GenBank under the accession number OR452190 The number of the isolates SDLC202109 is OR452191.

*Funding*

This work was supported by grants from the National Key R & D Program of China (2021YFF0703000).

*Acknowledgments*

We sincerely appreciate the support of the Innovation Team for Pig

Digestive Tract Infectious Diseases, the State Key Laboratory for Animal Disease Control and Prevention, the Harbin Veterinary Research Institute, and the Chinese Academy of Agricultural Sciences.

## Supplementary materials

Supplementary material associated with this article can be found, in the online version, at doi:10.1016/j.virusres.2023.199247.

## References


Anouja, F., Wattiez, R., Mousset, S., Caillet-Fauquet, P., 1997. The cytotoxicity of the parvovirus minute virus of mice nonstructural protein NS1 is related to changes in the synthesis and phosphorylation of cell proteins. J. Virol. 71, 4671–4678. https://doi.org/10.1128/jvi.71.6.4671-4678.1997.

Astell, C.R., Chow, M.B., n.d. Sequence analysis of the termini of virion and replicative forms of minute virus of mice DNA suggests a modified rolling hairpin model for autonomous parvovirus DNA replication. J. Virol. 54(1), 171–177. https://doi.org/10.1128/JVI.54.1.171-177.1985.

Astell, C.R., Chow, M.B., Ward, D.C., 1985. Sequence analysis of the termini of virion and replicative forms of minute virus of mice DNA suggests a modified rolling hairpin model for autonomous parvovirus DNA replication. J. Virol. 54, 171–177. https://doi.org/10.1128/JVI.54.1.171-177.1985.

Bergeron, J., Hébert, B., Tijssen, P., 1996. Genome organization of the Kresse strain of porcine parvovirus: identification of the allotropic determinant and comparison with those of NADL-2 and field isolates. J. Virol. 70, 2508–2515. https://doi.org/10.1128/jvi.70.4.2508-2515.1996.

Bergeron, J., Menezes, J., Tijssen, P., 1993. Genomic organization and mapping of transcription and translation products of the NADL-2 strain of porcine parvovirus. Virology 197, 86–98. https://doi.org/10.1006/viro.1993.1569.

Cadar, D., Dán, Á., Tombácz, K., Lőrincz, M., Kiss, T., Becskei, Z., Spînu, M., Tuboly, T., Cságola, A., 2012. Phylogeny and evolutionary genetics of porcine parvovirus in wild boars. Infect. Genet. Evol. 12, 1163–1171. https://doi.org/10.1016/j.meegid.2012.04.020.

Cartwright, S.F., Lucas, M., Huck, R.A., 1969. A small haemagglutinating porcine DNA virus. I. Isolation and properties. J. Comp. Pathol. 79, 371–377. https://doi.org/10.1016/0021-9975(69)90053-x.

Cavalier-Smith, T., 1974. Palindromic base sequences and replication of eukaryote chromosome ends. Nature 250, 467–470. https://doi.org/10.1038/250467a0.

Chapman, M.S., Rossmann, M.G., 1993. Structure, sequence, and function correlations among parvoviruses. Virology 194, 491–508. https://doi.org/10.1006/viro.1993.1288.

Chen, K.C., Shull, B.C., Moses, E.A., Lederman, M., Stout, E.R., Bates, R.C., 1986. Complete nucleotide sequence and genome organization of bovine parvovirus. J. Virol. 60, 1085–1097. https://doi.org/10.1128/JVI.60.3.1085-1097.1986.

Cotmore, S.F., Tattersall, P., 1987. The autonomously replicating parvoviruses of vertebrates. Adv. Virus Res. 33, 91–174. https://doi.org/10.1016/s0065-3527(08)60317-6.

Cui, J., Wang, X., Ren, Y., Cui, S., Li, G., Ren, X., 2012. Genome sequence of Chinese porcine parvovirus strain PPV2010. J. Virol. 86, 2379. https://doi.org/10.1128/JVI.06852-11.

De Souza, A.R., Yamin, M., Gava, D., Zanella, J.R.C., Gatti, M.S.V., Bonafe, C.F.S., De Lima Neto, D.F., 2019. Porcine parvovirus VP1/VP2 on a time series epitope mapping: exploring the effects of high hydrostatic pressure on the immune recognition of antigens. Virol. J. 16, 75. https://doi.org/10.1186/s12985-019-1165-1.

Deng, S., Zhiyong, H., Mengjiao, Z., Shuangqi, F., Jingyuan, Z., Yunzhen, H., Hailuan, X., Jinding, C., 2020. Isolation and phylogenetic analysis of a new Porcine parvovirus strain GD2013 in China. J. Virol. Methods 275, 113748. https://doi.org/10.1016/j.jviromet.2019.113748.

Duffy, S., Shackelton, L.A., Holmes, E.C., 2008. Rates of evolutionary change in viruses: patterns and determinants. Nat. Rev. Genet. 9, 267–276. https://doi.org/10.1038/nrg2323.

Dunne, H.W., Gobble, J.L., Hokanson, J.F., Kradel, D.C., Bubash, G.R., 1965. Porcine reproductive failure associated with a newly identified "SMEDI" group of picorna viruses. Am. J. Vet. Res. 26, 1284–1297.

Fernandes, S., Boisvert, M., Szelei, J., Tijssen, P., 2014. Differential replication of two porcine parvovirus strains in bovine cell lines ensues from initial DNA processing and NS1 expression. J. Gen. Virol. 95, 910–921. https://doi.org/10.1099/vir.0.059741-0.

Fernandes, S., Boisvert, M., Tijssen, P., 2011. Genetic elements in the VP region of porcine parvovirus are critical to replication efficiency in cell culture. J. Virol. 85, 3025–3029. https://doi.org/10.1128/JVI.02215-10.

Franzo, G., Zerbo, H.L., Ouoba, B.L., Dji-Tombo, A.D., Kindo, M.G., Sawadogo, R., Chang'a, J., Bitanyi, S., Kamigwe, A., Mayenga, C., Lo, M.M., Ndiaye, M., Ba, A., Diop, G.L., Anahory, I.V., Mapaco, L.P., Achá, S.J., Kouakou, V.K., Couacy-Hymann, E., Gacheru, S.G., Lichoti, J.K., Kasivalu, J.K., Njagi, O.N., Settypalli, T.B. K., Cattoli, G., Lamien, C.E., Molini, U., Dundon, W.G., 2023. A phylogeographic analysis of porcine parvovirus 1 in Africa. Viruses 15, 207. https://doi.org/10.3390/v15010207.

Gillick, J.C., 1977. An outbreak of swine foetal mummification associated with porcine parvovirus. Aust. Vet. J. 53, 105–106. https://doi.org/10.1111/j.1751-0813.1977.tb14903.x.

Hanson, N.D., Rhode, S.L., 1991. Parvovirus NS1 stimulates P4 expression by interaction with the terminal repeats and through DNA amplification. J. Virol. 65, 4325–4333. https://doi.org/10.1128/jvi.65.8.4325-4333.1991.

Hao, X., Lu, Z., Sun, P., Fu, Y., Cao, Y., Li, P., Bai, X., Bao, H., Xie, B., Chen, Y., Li, D., Liu, Z., 2011. Phylogenetic analysis of porcine parvoviruses from swine samples in China. Virol. J. 8, 320. https://doi.org/10.1186/1743-422X-8-320.

Johnson, R.H., 1973. Isolation of swine parvovirus in Queensland. Aust. Vet. J. 49, 157–159. https://doi.org/10.1111/j.1751-0813.1973.tb06768.x.

Johnson, R.H., Collings, D.F., 1969. Experimental infection of piglets and pregnant gilts with a parvovirus. Vet. Rec. 85, 446–447. https://doi.org/10.1136/vr.85.16.446.

Kamstrup, S., Langeveld, J., Bøtner, A., Nielsen, J., Schaaper, W.M.M., Boshuizen, R.S., Casal, J.I., Højrup, P., Vela, C., Meloen, R., Dalsgaard, K., 1998. Mapping the antigenic structure of porcine parvovirus at the level of peptides. Virus Res. 53, 163–173. https://doi.org/10.1016/S0168-1702(97)00145-7.

Li, J., Xiao, Y., Qiu, M., Li, Xinshuai, Li, S., Lin, H., Li, Xiangdong, Zhu, J., Chen, N., 2021. A systematic investigation unveils high coinfection status of porcine parvovirus types 1 through 7 in China from 2016 to 2020. Microbiol. Spectr. 9, e0129421 https://doi.org/10.1128/Spectrum.01294-21.

López-Bueno, A., Villarreal, L.P., Almendral, J.M., 2006. Parvovirus variation for disease: a difference with RNA viruses? In: Domingo, E. (Ed.), Quasispecies: Concept and Implications For virology, Current Topics in Microbiology and Immunology. Springer Berlin Heidelberg, Berlin, Heidelberg, pp. 349–370. https://doi.org/10.1007/3-540-26397-7_13.

Lukashov, V.V., Goudsmit, J., 2001. Evolutionary relationships among parvoviruses: virus-host coevolution among autonomous primate parvoviruses and links between adeno-associated and avian parvoviruses. J. Virol. 75, 2729–2740. https://doi.org/10.1128/JVI.75.6.2729-2740.2001.

Martínez, C., Dalsgaard, K., López De Turiso, J., Cortés, E., Vela, C., Casal, J., 1992. Production of porcine parvovirus empty capsids with high immunogenic activity. Vaccine 10, 684–690. https://doi.org/10.1016/0264-410X(92)90090-7.

Mengeling, W.L., 1979. Prenatal infection following maternal exposure to porcine parvovirus on either the seventh or fourteenth day of gestation. Can. J. Comp. Med. 43 (1), 106–109.

Molitor, T.W., Joo, H.S., Collett, M.S., 1983. Porcine parvovirus: virus purification and structural and antigenic properties of virion polypeptides. J. Virol. 45, 842–854. https://doi.org/10.1128/jvi.45.2.842-854.1983.

Oh, W.-T., Kim, R.-Y., Nguyen, V.-G., Chung, H.-C., Park, B.-K., 2017. Perspectives on the evolution of porcine parvovirus. Viruses 9, 196. https://doi.org/10.3390/v9080196.

Paradiso, P.R., 1984. Identification of multiple forms of the noncapsid parvovirus protein NCVP1 in H-1 parvovirus-infected cells. J. Virol. 52, 82–87. https://doi.org/10.1128/JVI.52.1.82-87.1984.

Parthiban, S., Sowndhraya, R.K.V., Raja, P., Parthiban, M., Ramesh, A., Raj, G.D., Senthilkumar, K., Balasubramanyam, D., Hemalatha, S., Bharathi, R., Ravishankar, C., Parveen, S.T., 2022. Molecular detection of porcine parvovirus 1–associated reproductive failure in southern India. Trop. Anim. Health Prod. 54, 195. https://doi.org/10.1007/s11250-022-03194-8.

Ranz, A.I., Manclús, J.J., Díaz-Aroca, E., Casal, J.I., 1989. Porcine parvovirus: DNA sequence and genome organization. J. Gen. Virol. 70 (Pt 10), 2541–2553. https://doi.org/10.1099/0022-1317-70-10-2541.

Ren, X., Tao, Y., Cui, J., Suo, S., Cong, Y., Tijssen, P., 2013. Phylogeny and evolution of porcine parvovirus. Virus Res. 178, 392–397. https://doi.org/10.1016/j.virusres.2013.09.014.

Rhode, S.L., 1989. Both excision and replication of cloned autonomous parvovirus DNA require the NS1 (rep) protein. J. Virol. 63, 4249–4256. https://doi.org/10.1128/jvi.63.10.4249-4256.1989.

Rhode, S.L., 1985. Nucleotide sequence of the coat protein gene of canine parvovirus. J. Virol. 54, 630–633. https://doi.org/10.1128/JVI.54.2.630-633.1985.

Sachs, A.B., 1993. Messenger RNA degradation in eukaryotes. Cell 74, 413–421. https://doi.org/10.1016/0092-8674(93)80043-e.

Shangjin, C., Cortey, M., Segalés, J., 2009. Phylogeny and evolution of the NS1 and VP1/VP2 gene sequences from porcine parvovirus. Virus Res. 140, 209–215. https://doi.org/10.1016/j.virusres.2008.11.003.

Simpson, A.A., Hébert, B., Sullivan, G.M., Parrish, C.R., Zádori, Z., Tijssen, P., Rossmann, M.G., 2002. The structure of porcine parvovirus: comparison with related viruses. J. Mol. Biol. 315, 1189–1198. https://doi.org/10.1006/jmbi.2001.5319.

Soares, R.M., Cortez, A., Heinemann, M.B., Sakamoto, S.M., Martins, V.G., Bacci, M., De Campos Fernandes, F.M., Richtzenhain, L.J., 2003. Genetic variability of porcine parvovirus isolates revealed by analysis of partial sequences of the structural coding gene VP2. J. Gen. Virol. 84, 1505–1515. https://doi.org/10.1099/vir.0.19011-0.

Soares, R.M., Durigon, E.L., Bersano, J.G., Richtzenhain, L.J., 1999. Detection of porcine parvovirus DNA by the polymerase chain reaction assay using primers to the highly conserved nonstructural protein gene, NS-1. J. Virol. Methods 78, 191–198. https://doi.org/10.1016/s0166-0934(98)00177-3.

Strassheim, M.L., Gruenberg, A., Veijalainen, P., Sgro, J.Y., Parrish, C.R., 1994. Two dominant neutralizing antigenic determinants of canine parvovirus are found on the threefold spike of the virus capsid. Virology 198, 175–184. https://doi.org/10.1006/viro.1994.1020.

Streck, A.F., Bonatto, S.L., Homeier, T., Souza, C.K., Gonçalves, K.R., Gava, D., Canal, C. W., Truyen, U., 2011. High rate of viral evolution in the capsid protein of porcine parvovirus. J. Gen. Virol. 92, 2628–2636. https://doi.org/10.1099/vir.0.033662-0.

Streck, A.F., Canal, C.W., Truyen, U., 2022. Viral fitness and antigenic determinants of porcine parvovirus at the amino acid level of the capsid protein. J. Virol. 96, e0119821 https://doi.org/10.1128/JVI.01198-21.

Streck, A.F., Canal, C.W., Truyen, U., 2015. Molecular epidemiology and evolution of porcine parvoviruses. Infect. Genet. Evol. 36, 300–306. https://doi.org/10.1016/j.meegid.2015.10.007.

Su, Q.-L., Li, B., Zhao, W., Liang, J.-X., He, Y., Qin, Y.-B., Lu, B.-X., 2015. Complete genome sequence of porcine parvovirus N strain isolated from Guangxi. China. Genome Announc. 3, e01359. https://doi.org/10.1128/genomeA.01359-14.

Vasudevacharya, J., Compans, R.W., 1992. The NS and capsid genes determine the host range of porcine parvovirus. Virology 187, 515–524. https://doi.org/10.1016/0042-6822(92)90454-W.

Vereecke, N., Kvisgaard, L.K., Baele, G., Boone, C., Kunze, M., Larsen, L.E., Theuns, S., Nauwynck, H., 2022. Molecular epidemiology of porcine parvovirus type 1 (PPV1) and the reactivity of vaccine-induced antisera against historical and current PPV1 strains. Virus Evol. 8, veac053. https://doi.org/10.1093/ve/veac053.

Wang, L.-Q., Wang, Y., Chen, L.-B., Fu, P.-F., Chen, H.-Y., Cui, B.-A., 2014. Complete genome sequence of a Porcine Parvovirus Strain isolated in Central China. Genome Announc 2, e01247. https://doi.org/10.1128/genomeA.01247-13.

Xu, Y.G., Cui, L.C., Wang, H.W., Huo, G.C., Li, S.L., 2013. Characterization of the capsid protein VP2 gene of a virulent strain NE/09 of porcine parvovirus isolated in China. Res. Vet. Sci. 94, 219–224. https://doi.org/10.1016/j.rvsc.2012.09.003.

Yu, Y., Zhang, J., Wang, J., Xi, J., Zhang, X., Li, P., Liu, Y., Liu, W., 2019. Naturally-occurring right terminal hairpin mutations in three genotypes of canine parvovirus (CPV-2a, CPV-2b and CPV-2c) have no effect on their growth characteristics. Virus Res. 261, 31–36. https://doi.org/10.1016/j.virusres.2018.12.007.

Zádori, Z., Szelei, J., Tijssen, P., 2005. SAT: a Late NS protein of porcine parvovirus. J. Virol. 79, 13129–13138. https://doi.org/10.1128/JVI.79.20.13129-13138.2005.

Zeeuw, E.J.L., Leinecker, N., Herwig, V., Selbitz, H.-J., Truyen, U., 2007. Study of the virulence and cross-neutralization capability of recent porcine parvovirus field isolates and vaccine viruses in experimentally infected pregnant gilts. J. Gen. Virol. 88, 420–427. https://doi.org/10.1099/vir.0.82302-0.

Zimmermann, P., Ritzmann, M., Selbitz, H.-J., Heinritzi, K., Truyen, U., 2006. VP1 sequences of German porcine parvovirus isolates define two genetic lineages. J. Gen. Virol. 87, 295–301. https://doi.org/10.1099/vir.0.81086-0.